See discussions, stats, and author profiles for this publication at: https://www.researchgate.net/publication/6600378

## Lateral Intermolecular Forces between Biomembrane Lipids in Two Dimensions: 1,2-Dipalmitin at the Heptane/Water Interface Compared with Phospholipids

ARTICLE in THE JOURNAL OF PHYSICAL CHEMISTRY B · FEBRUARY 2007

Impact Factor: 3.3 · DOI: 10.1021/jp0658748 · Source: PubMed

CITATIONS READS

3

## 2 AUTHORS:



Norman Pallas

Monsanto Company

16 PUBLICATIONS 518 CITATIONS

SEE PROFILE



Brian A Pethica

**Princeton University** 

172 PUBLICATIONS 3,824 CITATIONS

SEE PROFILE

# Lateral Intermolecular Forces between Biomembrane Lipids in Two Dimensions: 1,2-Dipalmitin at the Heptane/Water Interface Compared with Phospholipids

Norman R. Pallas<sup>†,‡</sup> and Brian A. Pethica\*,§

Monsanto Corp., 800 North Lindbergh Boulevard, St. Louis, Missouri 63167, and Department of Chemical Engineering, Princeton University, Princeton, New Jersey 08544

Received: September 8, 2006; In Final Form: October 31, 2006

The lateral interaction forces between phospholipids in two-dimensional arrays are fundamental to understanding membrane biophysics. In previous studies the related thermodynamic functions have been measured for spread phospholipid monolayers at the oil/water interface over a range of temperatures and densities, and the twodimensional virial coefficients obtained. These coefficients have been computed from a model that emphasizes the head group zwitterion interactions. In this study we examine the contribution of the diglyceride portion of phospholipid molecules to the lateral intermolecular forces. Measurements of the heptane/water interfacial tension as a function of the concentration of 1,2-dipalmitoyl glycerol (DP) in the heptane were made over a range of low surface pressures at 25 °C. Infrared measurements on the DP solutions show that the solutions are ideal. The results are interpreted to give two-dimensional virial coefficients for the adsorbed monolayer. The second virial coefficient  $B_2(T)$  for DP is  $\pm 0.31$  nm<sup>2</sup>/molecule, in marked contrast to the much larger positive values found for the corresponding phospholipids at the same interface and temperature, and clearly indicating an attractive component to the lateral potentials of mean force between pairs of DP molecules. The contribution of the diglyceride moiety to the pair potentials of the phospholipids thus appears to be minor but not negligible. The differences in the second virial coefficients for DP and the phospholipids are interpreted primarily in terms of the orientation of the ester carbonyl dipoles, also drawing on spectroscopic and diffraction evidence from related structures.

#### Introduction

The lateral interaction forces between phospholipid molecules in adsorbed or spread monolayers are directly relevant to understanding the cohesional forces between the structural components of biomembranes, in which phospholipids play an important role. Extensive thermodynamic data are available for a range of phospholipid monolayers spread at the heptane/water interface and other alkane/water interfaces. 1-8 The results for spread monolayers at low surface densities of phosphatidyl cholines and serines with several n-alkanoyl chain lengths at the heptane/water interface have been analyzed to give the twodimensional (2D) virial coefficients for these molecules over a range of temperatures. The results show, in particular, that the phospholipid second virial coefficients are surprisingly large and positive, increasing strongly with temperature, indicating substantial overall net repulsive pair potentials.9 The virial coefficients have been interpreted in a statistical mechanical model largely in terms of the lateral interactions of the zwitterionic head groups, with good agreement with the experimental results. 10 The component of the interaction force arising from the 1,2-dialkanoyl glycerol portion of these phospholipids plays a minor role in this model, which implies that the two large dipoles of the ester carbonyl groups-which are most likely to be on the heptane side of the interface—are so arranged at low monolayer densities as to give a negligible contribution to the potentials between phospholipid pairs. The

§ Princeton University.

purpose of this paper is to test this aspect of the model directly by obtaining the 2D virial coefficients for low-density monolayers of 1,2-dipalmitoyl glycerol molecules at the heptane/water interface for comparison with the phospholipid data.

There has been recent interest in two-dimensional virial coefficients in lipid monolayers at the A/W interface as the classical statistical mechanical route to lateral intermolecular forces between molecules (see ref 11 and 12 and the papers cited therein). Monolayers at oil/water (O/W) interfaces are less studied, but are of particular thermodynamic interest since the attractive forces between the alkyl chains are much attenuated as compared to the air/water (A/W) interface. This makes possible measurements with phospholipids at low surface densities at surface pressures at least a magnitude higher than at the A/W interface at comparable surface densities. The 2D virial coefficients are then available if surface pressure measurements are pursued in dilute monolayers to 1 mN m<sup>-1</sup> and lower. Apart from the body of information on the phospholipids summarized above, there are few low surface pressure isotherm studies on lipid monolayers at O/W interfaces adequate for estimating 2D virial coefficients from monolayer isotherms, which are mostly interpreted via equations of state. 13-18

Mono- and diglycerides are surface active in oil/water systems, as for example in numerous emulsions including those found in post-prandial fat absorption from the duodenum. There appear to be no data at low surface pressures for O/W monolayers of glycerides adequate for estimating virial coefficients. For example, the extensive data of Hayami and Motamura<sup>17,18</sup> on monoglycerides adsorbed at the hexane/water interface do not go to sufficiently low pressures to give the virial

<sup>\*</sup> Address correspondence to this author. E-mail: bpethica@princeton.edu.

<sup>†</sup> Monsanto Corp.

<sup>&</sup>lt;sup>‡</sup> Present Address: 3647, McDonald Ave., St. Louis, MO 63116.

coefficients directly, and possible association in the oil phase is not considered.

#### **Materials and Methods**

Pure *n*-heptane (HPLC grade, 99+%; low UV adsorption) was obtained from Aldrich Chemical Co. in multiple sealed 100 mL volumes packed under nitrogen and used as received. Each sample of heptane was used completely after opening. Samples of 1,2-dipalmitoyl-sn-glycerol (>99%, substantially free of the 1,3 isomer) were obtained from Fluka and stored cold. Successive samples as required were warmed to room temperature in a desiccator before opening to avoid condensation of water vapor on the dry powder. The ampules of heptane were opened without contact with fingers, the contents of the first ampule being used to wash-off the outside of the later ampules prior to opening. The required solutions in heptane were prepared volumetrically from stock solutions by successive dilution into 50 mL class A volumetric flasks, using class A pipets. The stock solutions were prepared in 100 mL class A volumetric flasks by weighing DP aliquots on an analytical balance, precise to  $\pm 0.1$  mg. Concentrations are recorded as molarities (M) at 25 °C. All capped containers of DP solutions were stored in a clean desiccator containing liquid heptane to suppress evaporation from the solutions. No degradation was found over the course of the measurements by comparing tension measurements on solutions as old as 1 month against fresh samples made from the same and new stock solutions.

Ultrapure water was obtained by passing house-grade deionized water though a Nanopure system of filters. All glassware and accessory materials were prepared and cleaned as has been described for the critical examination of the surface physical properties of insoluble films and the accurate use of the drop shape apparatus. 19-22

Interfacial tension was measured by drop-shape analysis with a Data Physics instrument purchased from Future Digital Scientific Corp. Since the general method has been well described in the literature<sup>20,21</sup> only a few comments will be made here. This particular commercial version uses the maximum gradient edge detection method, which is prone to occasional error, especially when internal reflections cause asymmetric shadows and bright areas within the drop. A simple alteration of the relative positioning of the drop with respect to the light source and CCD (charge coupled device) camera eliminates this problem. The lowest light level that provided good contrast avoided effects due to "bloom" as determined by direct examination of a drop and multiple estimations of the magnification factor, as determined by examination of NIST standard rods of calibrated dimensions. Multiple determinations with rods of different diameters demonstrated the absence of optical distortion and gave a magnification error estimate of 0.002%. Several improvements were made to the apparatus after extensive testing of the optics, orthogonality, magnification, alignments, mechanical traverse, and materials. The optical cell and thermostat (with windows) were replaced, using better optical windows to eliminate small distortions and effects found on changing the alignments required during measurement. The original optical cell could not be cleaned aggressively with acids. In the modified apparatus, the aqueous phase was contained in a double-walled all-glass custom-built cell with optically flat windows. A Lauda constant temperature bath maintained the cell at  $25.0 \pm 0.01$  °C, measured on an NIST-calibrated platinum resistance thermometer. A Hamilton microliter syringe was used to produce and control heptane drops for drop-shape analysis. The syringe plunger drive and mounting system is similar to

that previously reported.<sup>20</sup> Inverted syringe tips of various diameters were prepared from different gauge stainless steel tubes cut and ground square on the end and carefully bent upward to avoid pinching the tube. Use of different size tips and different magnification factors for fluids of different tensions is highly recommended. As previously described, there is an ideal drop shape for which the fitting function error is minimized.<sup>21</sup> This ideal shape is easily obtained with the appropriate combination of drop volume and tip size.

The unstirred aqueous and heptane phases were in thermal contact for at least 3 h to establish equilibrium. Drops were formed slowly over a few seconds to avoid vibrational effects. Images of drops were then recorded at about 1 per second and analyzed immediately. No aging was observed over the course of a typical experiment of about 10-15 min, nor in several measurements out to 2 h. Each solution was examined with separate drops three times with different positioning and focus, giving a set of data for each drop at one concentration. The resulting interfacial tension values were analyzed by using JMP, a statistical analysis software package from the SAS Institute. Since the concentrations of DP are very low, the density of the solutions was taken as for heptane.

The concentrations of DP in heptane in these experiments are up to  $2.1 \times 10^{-4}$  M and association is unlikely. These concentrations are too low to test for nonideality by vapor pressure osmometry, but the question may be approached by FTIR measurement of the DP hydroxyl bands. FTIR analysis of the hydroxyl bands at 3536 and 3487 cm<sup>-1</sup> as a function of DP concentration in heptane was accordingly made in a 0.4 mm KBr cell in a Nicolet FTIR apparatus.

### Results

From several hundred measurements on individual drops, the surface tension of the water used in these experiments was 71.95  $\pm$  0.025 mN m<sup>-1</sup> (standard error at the 99% confidence interval) at 25.0 °C. This is in good agreement with values obtained by capillary rise, Wilhelmy plate, and drop-shape measurements. 20-22 Repeated individual drop measurements of the heptane/water interfacial tension at 25.0 °C gave a value of  $50.89 \pm 0.02$  mN m<sup>-1</sup>. This value is slightly above the 50.66 mN m<sup>-1</sup> value for highly purified heptane obtained by the Wilhelmy method by our collaborators. 2,3,23 Ivosevic et al. 24 from a partial review of the literature on the interfacial tensions of alkanes with water measured by several methods prefer 50.77 mN m<sup>-1</sup> for heptane at 25 °C. They do not cite the results referenced above, nor an early value of 50.85 mN m<sup>-1</sup> obtained with purified heptane by the drop-shape method.<sup>25</sup> This body of interfacial tension values has been challenged by Goebel and Lunkenheimer, 26 who used a commercial drop-shape apparatus at 22 °C indicating tensions for a range of alkanes of unstated purity approximately 1 mN m<sup>-1</sup> higher than given in the extensive literature.<sup>26</sup> These authors claim that earlier values were from impure alkanes. Examination of the literature gives many papers in which extensive purification of the alkanes was carried out, including the use of solid adsorbent columns as recommended by Goebel and Lunkenheimer. We believe the "new" values to be related to deficiencies in their commercial drop-shape apparatus, particularly with the optical focusing, which do not meet the criteria which have been discussed in detail.<sup>20,21</sup> Since their paper appeared, a new set of data on the O/W interfacial tensions for a range of alkanes over a wide temperature range has been given by Zeppieri et al. using the drop-shape method.<sup>27</sup> These results are in sharp contrast with the claims of Goebel and Lunkenheimer, and give a value for heptane/water of 50.8 mN m<sup>-1</sup> at

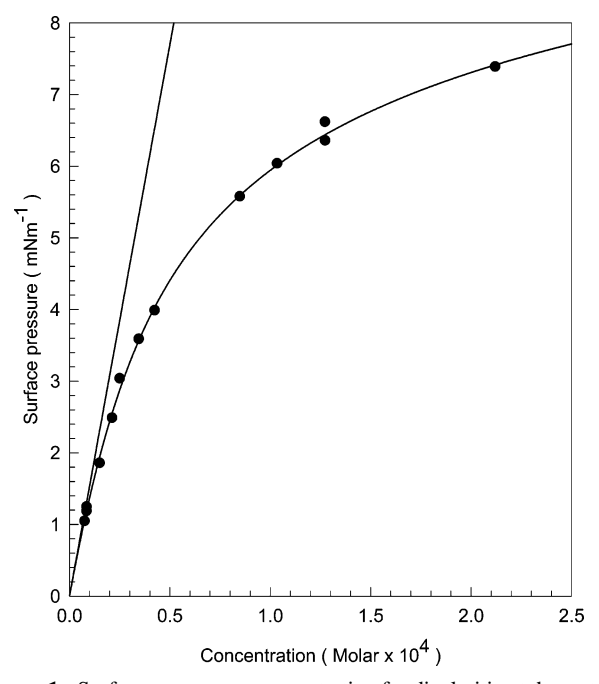


**Figure 1.** Surface pressure vs concentration for dipalmitin at the water/heptane interface at 25 °C. The line through the data points is drawn by using the values of the virial coefficients given in Table 1. The straight line is for  $\alpha = 1.543 \times 10^5$  mN m<sup>-1</sup> M<sup>-1</sup>.

25 °C, as read from their Figure 4. The agreement with the result presented here is excellent, and the claims of Goebel and Lunkenheimer can accordingly be rejected. We may also note than one of the well-known criteria of alkane purity, correctly adopted by these authors, the absence of time effects, is clearly exemplified in the present study.

The interfacial tension measurements of DP solutions in heptane are displayed as the surface pressure ( $\Pi$ ) as a function of concentration in Figure 1. As in all the figures showing the experimental data the lines drawn are from the values of the virial coefficients in the pressure expansion, as discussed below and shown in Table 1. The error in  $\Pi$  values is estimated to be not more than  $\pm 0.15$  mN m<sup>-1</sup>. A potential weakness of the experiments reported here is that the DP (>99%) and heptane (HLPC grade) were used as received. No interference with these measurements is anticipated from trace impurities in the heptane, which shows very small absorption in the UV and an interfacial tension just above previously accepted and more recent values with no observed time effects. From the method of synthesis of the DP,<sup>28</sup> monoglyceride and palmitic acid are possible interfering contaminants. Chromatographic analysis gave a DP

TABLE 1. a

	dipalmitin	lecithins	cephalins
$B_2(T)$ , nm <sup>2</sup> /molecule $B_3(T)$ , nm <sup>4</sup> /molecule <sup>2</sup> $B_4(T)$ , nm <sup>6</sup> /molecule <sup>3</sup>	0.31 <sub>3</sub> 0.077 0.073	2.27 3.12 -1.41	1.2 2.1 -0.7
B', nm²/molecule $C'$ , (nm²/molecule)(mN m $^{-1}$ ) $^{-1}$ $D'$ , (nm²/molecule)(mN m $^{-1}$ ) $^{-2}$	0.31 <sub>3</sub> 0.032 0.021		

<sup>a</sup> 2D virial coefficients for 1,2-dipalmitin (DP) and the n-alkyl phosphatidyl cholines (lecithins) and serines (cephalins) at the heptane/water interface at 25 °C. The data for lecithins are from Table 1 of ref 4. For cephalins, the values shown are averaged from the results (independent of NaCl concentration and temperature) in Table 2 of ref 4. Upper group: coefficients for the surface density expansion. Lower group: coefficients for the surface pressure expansion. Italics indicate tentative estimates of the magnitudes of the higher virial coefficients for dipalmitin monolayers (see text).

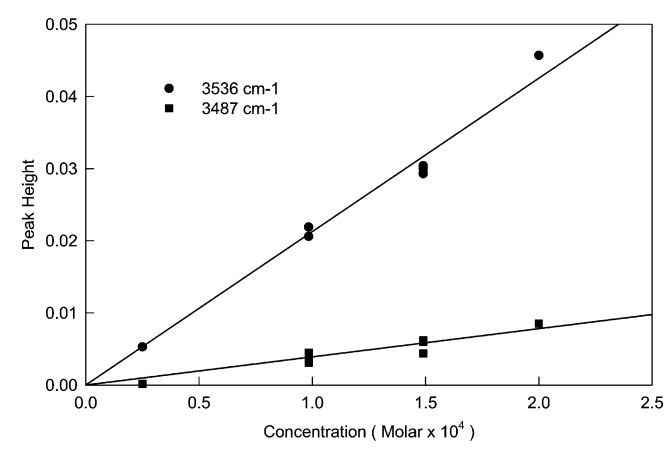


**Figure 2.** Infrared absorbance at two wavenumbers for dipalmitin in *n*-heptane in a 0.4 mm KBr cell.

purity of 99.3%, with no measurable monopalmitin and 0.7% w/w palmitic acid. The adsorption of monolaurin and monomyristin at the hexane/water interface has been measured at intermediate to higher pressures, showing surface activity decreasing modestly with chain length.<sup>17,18</sup> Extrapolation to the palmitin chain length shows that the surface activity of the monopalmitin, as indicated by the surface pressure at a given molar concentration in the range studied here, is about 40% of dipalmitin. On this basis, interference by trace monopalmitin with the pressure measurements given here will be completely negligible. The effect of palmitic acid dissolved in the oil phase on the O/W interfacial tension of hexadecane has been measured.<sup>29</sup> The surface activity is weak, with an initial slope of the  $\Pi$ -c plot of  $\sim 4 \times 10^3$  mN m<sup>-1</sup> M<sup>-1</sup> at 25 °C. The interfacial surface pressure of alkane-soluble long chain compounds at alkane/water interfaces depends modestly on the chain length of the alkane. 17,18,30-32 For long-chain alcohols, the initial slope increases by a factor of  $\sim 1.5$  from hexadecane to octane.<sup>31</sup> Correspondingly, at the highest DP concentration measured in the present study (2.5  $\times$  10<sup>-4</sup> M) a 0.7% palmitic acid contaminant would give an interfacial tension lowering of  $\sim 2.5$  $\times 10^{-2}$  mN m<sup>-1</sup>, at the limit of the sensitivity of our apparatus and below the reproducibility of our results. We accordingly may neglect any contribution to our measurements from palmitic acid. This conclusion is confirmed by the absence of measurable time effects up to 2 h.

The results of the FTIR study of the DP solutions are given in Figure 2. It was shown by Aveyard et al.14 for octanol and dodecanol in n-octane solution that deviations from ideality as observed by vapor-pressure osmometry correlate with the appearance of hydrogen-bonded dimers and larger clusters of the alcohol molecules, as identified from the changes in the hydroxyl IR absorption band. As shown in Figure 2, the IR absorption for DPG in heptane is linear with concentration over the experimental range at two frequencies with no evidence of dimerization. We conclude that the DP solutions may be treated as ideal. This conclusion is supported by the results of vaporpressure osmometry on long-chain alkanols in octane<sup>14</sup> and 1-monooleyl glycerol in heptane.<sup>31</sup> In these solutions, deviations from ideality due to hydrogen bonding are observed only at concentrations higher than  $\sim 10^{-3}$  M, well above the concentrations of DP in this study.

### **Data Analysis**

Estimation of the 2D virial coefficients follows the methods described earlier, <sup>12</sup> which can be summarized briefly. The virial

expansion in the surface density is given by

$$\Pi/kT = \Gamma + B_2(T)\Gamma^2 + B_3(T)\Gamma^3 + B_4(T)\Gamma^4 + \dots$$
 (1)

where k is Boltzmann's constant,  $\Gamma$  is the surface density of the monolayer species, and  $B_n(T)$  is the nth temperaturedependent virial coefficient, with  $B_1(T) = 1$ . Applying the Gibbs Adsorption Isotherm for ideal solutions, and rearranging

$$\Pi/kT = \sum B_n(T)[(c/kT) d\Pi/dc]^n$$

where c is the solute concentration. In practice the summation is truncated at the highest value of n consistent with the statistical limitations of the data. The second virial coefficient can be obtained from

$$B_2(T)/kT = -\beta/\alpha^2 \tag{2}$$

where  $\alpha = \lim d\Pi/dc$  and  $\beta = \lim d(\Pi/c)/dc$  as c goes to zero, estimated both by graphing and regression methods.

A parallel analysis utilizes the virial expansion in the surface pressure, treating the surface phase as pseudo-one-component. This is equivalent to the zero convention for the (heptane) solvent form of the Gibbs adsorption isotherm, with the water at constant chemical potential in view of the virtual insolubility of DP in the aqueous phase. The virial expansion in the pressure

$$\Pi A/kT = 1 + (B'\Pi + C'\Pi^2 + D'\Pi^3 + ...)/kT$$
 (3)

where A is the area/molecule of the adsorbed species and B', C', etc. are the temperature-dependent second, third, etc. virial coefficients in the pressure expansion. It is readily shown that  $B_2(T) = B'$ . For an ideal solution, the surface fugacity  $(\Pi^*)$  of the adsorbed monolayer is given by

$$\Pi^* = \alpha c = \Pi \exp(B'\Pi + C'\Pi^2/2 + D'\Pi^3/3 + ...)/kT$$
 (4)

noting that  $\Pi^*/\Pi$  goes to  $\alpha$  as c and  $\Pi$  go to zero.<sup>33</sup>

Figure 3 shows the experimental data plotted as  $ln(\Pi/c)$ against  $\Pi$ , which indicates directly from eq 4 that virial coefficients beyond the second are required to cover the data. Figure 4 shows the data plotted for the estimation of  $\alpha$  and  $\beta$ to be applied in eq 2. Since the parallel data analyses depend on the value of  $\alpha$ , the procedure adopted was first to obtain the best estimate for  $\alpha$  by comparing graphical and regression methods for analyzing the data as  $\Pi - c$ ,  $\ln(\Pi/c) - \Pi$ , and  $(\Pi/c) - \Pi$ c)-c relations as shown in Figures 1, 3, and 4. Since the  $\Pi$ -c plot must pass through zero, graphing with this plot readily gives a realistic range for  $\alpha$  of 1.55  $\pm$  0.03  $\times$  10<sup>5</sup> mN m<sup>-1</sup> M<sup>-1</sup>. The values for  $\alpha$  from the  $(\Pi/c)-c$  plot overlay this range but are less precise. Since  $\alpha$  and  $\beta$  are of opposite sign, increase of  $\alpha$ corresponds with an increase in  $-\beta$ , tending to compensate to reduce the variability of  $B_2(T)$  obtained from eq 2. Over the realistic range for  $\alpha$ ,  $B_2(T)$  is not sensitive to the choice of  $\alpha$ , with a resulting value of 0.313 nm<sup>2</sup>/molecule with a variation of  $\sim 1\%$ . Graphical estimates of  $\alpha$  from analysis of the semilogarithmic form of eq 4 give a spread overlapping the range apparent from the other two methods. Using the same plot gives values of B' sensitive to the choice of  $\alpha$ . Good correspondence between the methods is obtained by taking  $\alpha$ as  $1.543 \times 10^5 \text{ mN m}^{-1} \text{ M}^{-1}$ , which gives B' as  $0.313 \text{ nm}^2$ / molecule from both eq 2 and the semilogarithmic form of eq 4, in accord with the necessary requirement that  $B' = B_2(T)$ . We

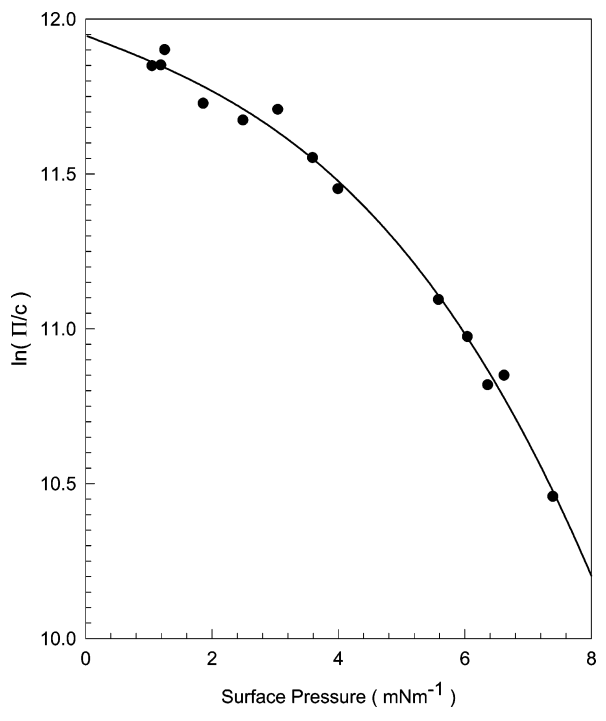


**Figure 3.** Ln( $\Pi/c$ ) vs  $\Pi$  for dipalmitin at the water/heptane interface at 25 °C. The line is drawn with the values of the virial coefficients shown in Table 1.

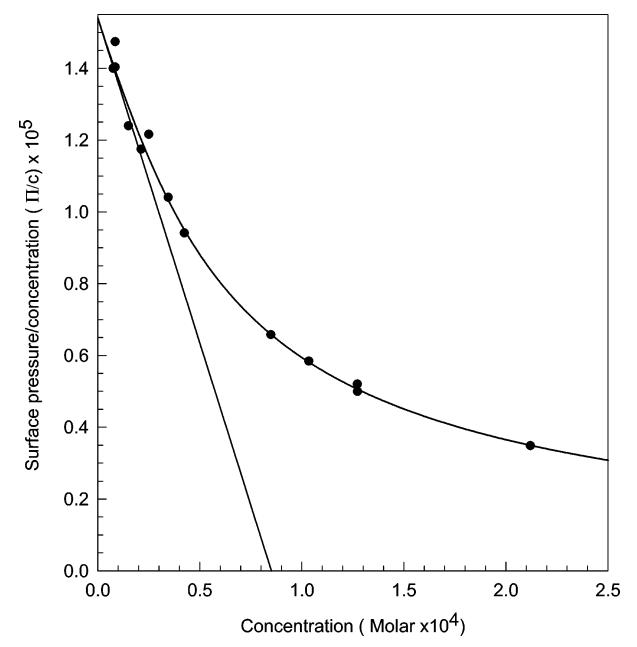


**Figure 4.**  $\Pi/c$  vs concentration for dipalmitin at the water/heptane interface at 25 °C. The line through the data points is drawn with the values of the virial coefficients shown in Table 1. The straight line shows the slope for  $\beta$  in eq 2.

conclude that  $B_2(T) = B' = 0.31_3 \text{ nm}^2/\text{molecule}$  is the appropriate best estimate for the second viral coefficient.

Estimates of the higher virial coefficients were then obtained by analysis of the differences at higher pressures between the experimental results and the pressures calculated by adopting the above  $\alpha$  and B' values in eq 4. The difference analysis shows an improvement in statistical fit up to the fourth coefficient. The data are sufficient to give a fair estimate for the third coefficient with the fourth plainly very approximate, not least for its dependence on the interfacial pressure at the last point at the highest DP concentration studied, which is close to the

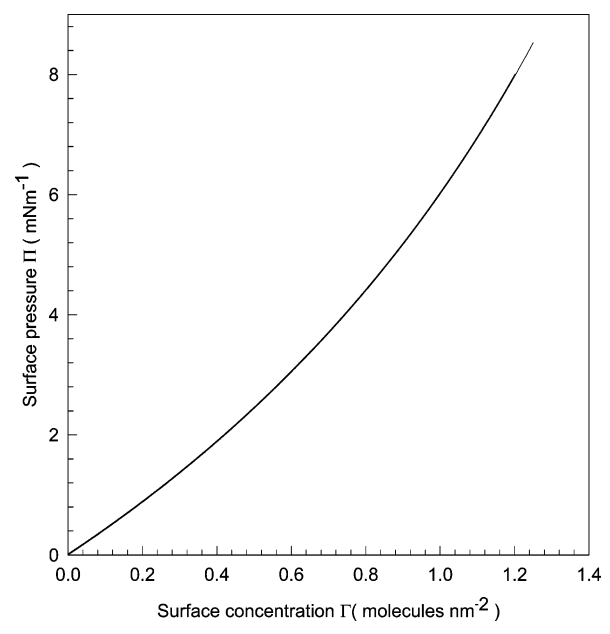


**Figure 5.** Surface pressure vs surface concentration isotherm for dipalmitin at the n-heptane/water interface at 25 °C.

saturation limit. Having located the range of coupled values for C' and D', the preferred values were obtained by the following procedure. From eq 4,  $\Pi$  was calculated from c by using the preferred  $\alpha$  and B' with a set of coupled C' and D' values in their estimated ranges. By close interpolation, calculated values of  $\Pi$  were obtained at each experimental value of c. The calculated and measured values of  $\Pi$  were then compared and the statistical fit obtained and displayed as an  $R^2$  landscape. The set giving the best  $R^2$  (0.99886) was identified and recorded in Table 1. This statistical procedure, using the  $R^2$  "landscape", has been discussed previously, and is adopted to avoid the error in using standard regression software on the logarithmic form of eq 4. Standard regression software assumes that the errors in the parameters being related are Gaussian. This is a valid assumption for  $c/\Pi$ , but not for the logarithm.  $^{12,34}$ 

By using these results, it is straightforward to use the Gibbs Adsorption Isotherm to establish the  $\Pi - \Gamma$  relationship for the adsorbed DP, as shown in Figure 5. This leads immediately from eq 1 to the higher virial coefficients in the density expansion. Standard regression with eq 1 indicates that the density expansion gives an excellent fit to the experimental data by truncation of the virial expansion at the fourth coefficient  $(R^2 = 0.999988)$  yielding the values of  $B_3(T)$  and  $B_4(T)$  shown in Table 1. This high  $R^2$  value is somewhat misleading since the  $R^2$  landscape around the chosen values is rather flat and the experimental error has not been expressly included in the statistics. Again, the fourth coefficient from this set of calculations is the least reliable. The  $\Pi$ - $\Gamma$  relationship shown in Figure 5 is calculated from both the density and pressure virial expansions, using the coefficients from Table 1. The two lines are almost identical, the difference being barely visible on the graph at the highest pressure and density only.

#### **Discussion**

The value of  $B' = B_2(T) = 0.31 \text{ nm}^2/\text{molecule}$  for dipalmitin at 25 °C is definitely less than the close-packed area of  $\sim 0.40$  typical for a pair of long hydrocarbon chains. The molecular areas of long-chain n-alkanoyl glycerides spread at the air/water (A/W) interface in the close-packed state at temperatures at or close to 25 °C are given as between 0.19 and 0.21 nm²/molecule

for 1-monoglycerides, 0.40 for 1,2-diglycerides, and 0.60 for triglycerides at high surface pressures near collapse.  $^{35-38}$  1,2-n-alkanoyl phospholipids spread at the heptane/water interface show areas at high pressures close to 0.44 nm²/molecule.  $^{1,4}$  For noninteracting hard discs,  $B_2(T)$  will be approximately twice the close-packed area, giving  $\sim$ 0.8 nm²/molecule for DP. Calculations for 1,2-n-alkylphosphatidyl choline head groups, taken as hard circular discs or as rectangles minicking the geometry of the zwittterion head groups, give values of  $B_2(T)$  of 0.892 and 0.972 nm²/molecule, respectively,  $^{39}$  compared to the close-packed area of 0.446 nm²/molecule. It follows from  $B_2(T) = 0.31$  that the lateral potential of mean force for DP molecule pairs in the adsorbed monolayers includes a significant attractive component that substantially reduces the positive value of the coefficient expected from the exclusion area alone.

If this attractive component is ascribed to the two DP ester groups, it follows that the carbonyl dipoles are probably in the oil phase and oriented more parallel than normal to the interface such that the intermolecular attraction from the free rotation of the ester dipole components tangential to the interface is larger than the repulsive effect of the normal components. Their orientation in both glyceride and phospholipid A/W monolayers depends on the surface density, as judged from surface potentials  $(\Delta V)$ . Surface potentials for phospholipid monolayers at the air/water and heptane/water interfaces indicate that the net dipole moment normal to the surface plane is constant at low surface densities, decreasing at higher densities. This decrease is a composite of the mutual polarization of the ester and zwitterion dipoles of the head groups and related changes in orientation of the adjacent water molecules.

Hydrogen bonding between the DP molecule pairs is a possible short-range attractive contributor to  $B_2(T)$  and could involve both the two ester carbonyls and the single hydroxyl group of the diglyceride. Hydrogen bonding to the ester groups is also possible for phospholipid molecular pairs, and is considered further below. We note that temperature effects will be particularly relevant to hydrogen bonding, and that the orientation of the ester carbonyl dipoles in both DP and phospholipids may be influenced by hydrogen bonding.

The positive  $B_2(T)$  values for phospholipids at the heptane/ water interface are much larger than those for DP, particularly for the dialkyl phosphatidyl cholines (lecithins), as shown in Table 1. The lecithins at 25 °C give  $B_2(T)$  as 2.27 nm<sup>2</sup>/molecule, independent of chain length and aqueous NaCl concentration, diminishing at lower temperatures to give 1.15 at 5 °C. The corresponding dialkyl phosphatidyl ethanolamines (cephalins) show  $B_2(T)$  values which vary little with temperature, <sup>9</sup> coinciding with the value for lecithin at 5  $^{\circ}$ C and  $\sim$ 20% larger than anticipated from the excluded area term alone. If the orientation and position of the carbonyl dipoles relative to the interface is similar in DP and the corresponding phospholipids in dilute monolayers, the data presented here certainly support the argument that the second virial coefficients for O/W phospholipid monolayers are predominantly explained by repulsion between the out-of-plane normal components of the head group zwitterions, with the cation closer to the interface than the phosphate group.<sup>10</sup> In particular, if the hydrophobic cation of lecithin is partially in the heptane phase to an extent increasing with temperature, the large temperature coefficient for the lecithin  $B_2(T)$  is explained.

From the NMR spectra of <sup>13</sup>C-labeled carbonyl groups of both dipalmitoyl lecithin and cephalin, the carbonyl conformations were shown to be similar in liquid crystals of mixtures containing 10% of each lipid in egg lecithin.<sup>44</sup> These results

suggest similar ester carbonyl conformations in dense DP and lecithin O/W monolayers, but may not apply to the dilute O/W monolayers in which the long alkyl chains are not conformationally confined as in the liquid crystal state. Further evidence on carbonyl dipole orientation in phospholipid crystals and liquid crystals as given by X-ray, NMR, and neutron scattering has been summarized by Stigter and Dill.<sup>39</sup> The carbonyl dipoles are largely oriented tangentially to the plane of the bilayer structures in these two crystalline states. If retained in dilute phospholipid O/W monolayers, this orientation will contribute an attractive component to the pair potentials. Short-range hydrogen bonding has also been considered as an attractive component of the pair potentials for phospholipid O/W monolayers.<sup>10</sup> Direct comparison of the role of hydrogen bonding for DP and phospholipids is constrained by the absence of hydroxyl groups in phosphatides and the potential for hydrogen bonding at the phosphate groups. Additional hydrogen bonding at the carboxyl and amino groups of the serine in cephalins is also possibly relevant.

If free rotation of the DP head groups in dilute monolayers does contribute a significant dipolar attractive component to the pair potential, a similar contribution will apply for phospholipid monolayers if the carbonyl orientations are similar. This implies that the model which successfully explains the large positive second virial coefficients for phospholipid monolayers<sup>10</sup> may modestly underestimate the out-of-plane orientation of the zwitterions of the head groups. Since hydrogen bonding is typically reduced at higher temperatures, it is noteworthy that  $B_2(T)$  for phosphatidyl serines is little affected by change in temperature, and that  $B_2(T)$  for the phosphatidyl cholines converges with the serine value at  $\sim$ 5 °C. Given the greater potential for hydrogen bonding for the serine group compared to choline, a major role for hydrogen bonding in defining the phospholipid pair potentials appears unlikely. Whether the twin carbonyl dipoles and hydrogen bonding contribute significantly to the lattice energies of the condensed phases of O/W monolayers of phospholipids where mutual intermolecular electrical polarization can be expected<sup>1</sup> remains to be seen.

For the higher virial coefficients we find C' = 0.032 (nm<sup>2</sup>/ molecule)(mN m<sup>-1</sup>)<sup>-1</sup> and D' = 0.021 (nm<sup>2</sup>/molecule)(mN  $(m^{-1})^{-2}$ . Analysis of the density expansion gives  $B_3(T) = 0.077$ nm<sup>4</sup>/molecule<sup>2</sup> and  $B_4(T) = 0.073$  nm<sup>6</sup>/molecule.<sup>3</sup> These estimates of the higher virial coefficients are given in Table 1, together with the coefficients for the phospholipids at 25 °C from Mingins et al.  $^9$  The values recorded for C' and D'—and consequently for  $B_3(T)$  and  $B_4(T)$ —must be regarded as preliminary since the value of  $R^2$  which indicates the quality of fit to the experimental results is not very sensitive to alternative nearby choices. Inclusion of the fourth coefficients inevitably improves the statistical fit, but the fourth coefficients recorded are particularly tentative since they depend on the single experimental point at the highest DP concentration. The values of  $B_3(T)$  for DP, lecithin, and cephalin are positive, with the DP value at 20–25% of the phospholipid values. For  $B_4(T)$  the sign is positive for DP and negative for the phospholipids.

#### Conclusions

From interfacial tension measurements at low surface pressures, the two-dimensional second virial coefficient for 1,2dipalmitoyl glycerol adsorbed at the heptane/water interface at 25 °C is shown to be positive with a value of +0.31<sub>3</sub> nm<sup>2</sup>/ molecule, much less than the second virial coefficient to be expected from the exclusion area alone, indicating a substantial attractive contribution to the lateral pair potential between DP

molecules in the monolayer. The attractive component of the potential of mean force of the DP molecular pairs can be ascribed to the rotation of the head groups with the ester carbonyls in a net orientation nearly parallel to the interface, or less probably to a short-range intermolecular hydrogen bonding. On the assumption that the headgroup orientation and position relative to the interface is similar in dilute heptane/water monolayers of glycerides and their related phospholipids, the value of  $B_2(T)$  for DP rules out any positive contribution from the ester carbonyl dipoles to the remarkably large positive second virials shown by dilute phospholipid monolayers, as accounted for in the model given by Mingins, Stigter, and Dill.<sup>9,10</sup> On the contrary, the results reinforce the basic feature of the model that the out-of-plane orientation of the phospholipids zwitterions is the prime cause of their large positive second virial coefficients, and that this effect may be somewhat larger than the model proposed. The third virial coefficient in the density expansion for DP is of the same positive sign as for the phopholipids but again smaller than that for the phospholipids. The fourth coefficient for DP is again positive, in contrast with a negative value for the phospholipids. Strong mutual polarization of the zwitterion dipoles will be a factor in defining the phospholipid virial coefficients for the higher clusters.

Acknowledgment. We wish to thank Monsanto for supporting this study and for permission to publish. We also thank Dr. J. Mingins for his critical comments and Betty Bautista of Unilever Research (Trumbull, CT) for the analysis of dipalmitin.

#### **References and Notes**

- (1) Mingins, J.; Pethica, B. A. Langmuir 2004, 20, 7493.
- (2) Brooks, J.; Pethica, B. A. Trans. Faraday Soc. 1964, 60, 208.
- (3) Brooks, J.; Pethica, B. A. Proc. Int. Congr. Surf. Act., 4th 1964, 2,
- (4) Yue, B.; Jackson, C. M.; Taylor, J. A. G.; Mingins, J.; Pethica, B. A. J. Chem. Soc., Faraday Trans. 1 1976, 72, 2685.
- (5) Taylor, J. A. G.; Mingins, J; Pethica, B. A. J. Chem. Soc., Faraday Trans. 1976, 72, 2694.
- (6) Mingins, J.; Taylor, J. A. G.; Pethica, B. A.; Jackson, C. M.; Yue, B. Y. T. J. Chem. Soc., Faraday Trans. 1982, 78, 323.
- (7) Pethica, B. A.; Mingins, J.; Taylor, J. A. G. J. Colloid Interface Sci. 1976, 55, 2.
- (8) Thoma, M.; Mohwald, H. J. J. Colloid. Interface Sci. 1994, 162, 340.
  - (9) Mingins, J.; Stigter, D.; Dill, K. A. Biophys. J. 1992, 61, 1603.
  - (10) Stigter, D.; Mingins, J.; Dill, K. A. Biophys. J. 1992, 61, 1616.
  - (11) Pethica, B. A.; Glasser, M. L. Langmuir 2005, 21, 944.
- (12) Pethica, B. A.; Glasser, M. L.; Cong, E. H. Langmuir 2003, 19,
- (13) Aveyard, A.; Chapman, J., Can. J. Chem. 1975, 53, 916.
- (14) Aveyard, R.; Briscoe, B. J.; Chapman, J. J. Chem. Soc., Faraday Trans. I 1973, 69, 1772.
- (15) Aveyard, R.; Briscoe, B. J.; Chapman, J. J. Colloid Interface Sci. 1973, 44, 282.
- (16) Takiue, T.; Matsuo, T.; Ikeda, N.; Motomura, K.; Aratono, M. J. Phys. Chem. B 1998, 102, 4911.
  - (17) Hayami, Y.; Motamura, K. J. Colloid Interface Sci. 1999, 209, 173. (18) Hayami, Y.; Motamura, K. J. Colloid Interface Sci. 1999, 220, 374.
- (19) Pallas, N. R.; Pethica, B. A. J. Chem. Soc., Faraday Trans. I 1987, 83, 585.
- (20) Pallas, N. R.; Harrison, Y. Colloid Surf. 1990, 69, 43.
- (21) Jennings, J. W., Jr.; Pallas, N. R. Langmuir 1988, 4, 959.
- (22) Pallas, N. R.; Pethica, B. A. Colloid Surf. 1983, 6, 221.
- (23) Mingins, J.; Owens, N. F.; Taylor, J. A. G.; Brooks, J.; Pethica, B. A. Adv. Chem. Ser. 1975, 144, 123.
  - (24) Ivosevic, N.; Zuric.V.; Tomaic, J. Langmuir 1999, 15, 7063.
  - (25) Bartell, F. E.; Davis, J. K. J. Phys. Chem. 1941, 45, 1321.
  - (26) Goebel, A; Lunkenheimer, K. Langmuir 1997, 13, 369.
- (27) Zeppieri, S.; Rodriguez, J.; Lopez de Ramos, A. L. J. Chem. Eng. Data 2001, 46, 1086.
- (28) Sowden, J. C.; Fischer, H. O. L. J. Am. Chem. Soc. 1941, 63, 3244. (29) Campanelli, J. R.; Wang, X. J. Colloid Interface Sci. 1999, 213,
- (30) Caminati, G.; Senatra, D.; Gabrielli, G. Langmuir 1991, 7 1969.

- (31) Aveyard, R; Briscoe, B. J. J. Chem. Soc., Faraday Trans. I 1972, 68, 478.
- (32) Andrews, D. M.; Manev, E. D.; Haydon, D. A. Special Discussions of the Faraday Society 1970, 1, 46.
- (33) Guggenheim, E. A. *Thermodynamics. An Advanced Treatise for Chemists and Physicists*, 2nd ed.; North Holland Publishing Co.: Amsterdam, The Netherlands, 1950; pp 88 and 99.
  - (34) Johnson, M. L. Anal. Biochem. 1992, 206, 215.
  - (35) Merker, D. R.: Daubert, B. F. J. Am. Chem. Soc. 1958, 80, 516.
  - (36) Merker, D. F.; Daubert, B. F. J. Am. Chem. Soc. 1964, 86, 1009.
- (37) Cadenhead, D. A.; Balthasar, D. M. J. Colloid Interface Sci. 1985, 107, 567.

- (38) Patino, J. M. R.; Dominguez, M. R. Colloid Surf. 2000, 168, 35.
- (39) Stigter, D; Dill, K. A. Langmuir 1988, 4, 200.
- (40) Standish, M. M.; Pethica, B. A. Trans. Faraday Soc. 1968, 64,
  - (41) Smaby;, J. M.; Brockman, H. L. Biophys. J. 1990, 58, 195.
- (42) Pethica, B. A.; Mingins, J.; Taylor, J. A. G. J. Colloid Interface Sci. 1976, 55, 2.
- (43) Vilallonga, R. F.; Garrett, E. R.; Cereijido, M. J. Pharm. Sci. 1972, 61, 1720.
- (44) Smith, S. S.; Kustanovich, I.; Shastri, B.; Salmon, A.; Hamilton, J. A. *Biochemistry* 1992, 31, 11660.